JOURNAL OF BACTERIOLOGY, Mar. 2002, p. 1359–1369 Vol. 184, No. 5
0021-9193/02/$04.00+0 DOI: 10.1128/JB.184.5.1359–1369.2002

Positive Growth Rate-Dependent Regulation of the *pdxA*, *ksgA*, and *pdxB* Genes of *Escherichia coli* K-12

Andrew J. Pease,† Benjamin R. Roa,‡ Wen Luo,§ and Malcolm E. Winkler*

Department of Microbiology and Molecular Genetics, University of Texas Houston Medical School, Houston, Texas 77030-1501

Received 13 July 2001/Accepted 2 November 2001

We found that transcription of the *pdxA* and *pdxB* genes, which mediate steps in the biosynthesis of the essential coenzyme pyridoxal 5′-phosphate, and the *ksgA* gene, which encodes an rRNA modification enzyme and is partly cotranscribed with *pdxA*, is subject to positive growth rate regulation in *Escherichia coli* K-12. The amounts of the *pdxA-ksgA* cotranscript and *pdxB*- and *ksgA*-specific transcripts and expression from *pdxA*- and *pdxB-lacZ* fusions increased as the growth rate increased. The half-lives of *ksgA*- and *pdxB*-specific transcripts were not affected by the growth rate, whereas the half-life of the *pdxA-ksgA* cotranscript was too short to be measured accurately. A method of normalization was applied to determine the amount of mRNA synthesized per gene and the rate of protein accumulation per gene. Normalization removed an apparent anomaly at fast growth rates and demonstrated that positive regulation of *pdxB* occurs at the level of transcription initiation over the whole range of growth rates tested. RNA polymerase limitation and autoregulation could not account for the positive growth rate regulation of *pdxA*, *pdxB*, and *ksgA* transcription. On the other hand, growth rate regulation of the amount of the *pdxA-ksgA* cotranscript was abolished by a *fis* mutation, suggesting a role for the Fis protein. In contrast, the *fis* mutation had no effect on *pdxB*- or *ksgA*-specific transcript amounts. The amounts of the *pdxA-ksgA* cotranscript and *ksgA*-specific transcript were repressed in the presence of high intracellular concentrations of guanosine tetraphosphate; however, this effect was independent of *relA* function for the *pdxA-ksgA* cotranscript. Amounts of the *pdxB*-specific transcript remained unchanged during amino acid starvation in wild-type and *relA* mutant strains.

Pyridoxal 5′-phosphate (PLP) is a ubiquitous coenzyme that plays fundamental roles in the metabolism of all cells (9, 16, 21, 31). One property that makes PLP such a versatile coenzyme is its ability to form reactive Schiff bases with amino groups (9, 16, 21, 31). Consequently, many classes of enzymes involved in amino acid metabolism use PLP as a coenzyme, including racemases, transaminases, decarboxylases, oxidative deaminases, and enzymes that replace side chains in or eliminate side chains from carbon atoms (9, 16, 21, 31). In addition, PLP is the essential coenzyme of glycogen phosphorylases, where PLP is thought to act in acid-base catalysis, which is a completely different mechanism from its reactions with amino groups (29).

Intracellular PLP amounts appear to be regulated in *E. coli*, and deprivation or overproduction of PLP has deleterious effects on bacterial cell physiology and growth (9, 18, 19, 36, 39), although this regulation is incompletely understood. Moreover, recent findings suggest that de novo PLP biosynthesis occurs by two distinct pathways in different organisms (23, 30, 48, 51, 74). The well-characterized pathway found in *E. coli* is present in some bacterial species (48, 74), whereas other bacteria, fungi, and plants possess a recently discovered pathway that is largely uncharacterized (23, 48, 51). The same salvage pathway seems to be present in all organisms (16, 19, 21, 30, 74).

Most of the genes involved in the de novo biosynthesis of PLP in *E. coli* are located in multifunctional superoperons (74). The arrangements of the *pdxA* and *pdxB* genes that are the subject of this report are depicted in Fig. 1. *pdxA* encodes NAD^+-dependent 4-hydroxythreonine 4-phosphate dehydrogenase, which synthesizes a substrate that is condensed with 1-deoxy-D-xylulose 5-phosphate by the PdxJ enzyme to form pyridoxine (PN) phosphate (PNP), which is the first B_6 vitamer synthesized by the de novo pathway (11, 12, 26, 38, 77, 78). *pdxA* is located in a complex superoperon with *surA* (periplasmic peptidyl-prolyl isomerase; stationary-phase survival) and *ksgA* 16S rRNA methyltransferase (55, 66, 73; Fig. 1A). *surA* and *pdxA* are cotranscribed, and insertion mutations in *surA* cause PN auxotrophy (66). The transcription start and promoter upstream of *surA-pdxA* were preliminarily mapped at P_{surA} (Fig. 1A), and there is evidence for a minor promoter at P_{pdxA} (Fig. 1A) (R. Kolter, personal communication). Work is under way to definitively map the promoters for the *pdxA* superoperon and determine which promoter(s) is regulated. About half of the amount of the *ksgA* transcript detected in exponentially growing cells is present in a *surA-pdxA-ksgA* cotranscript (55). The rest of the *ksgA* transcripts arise from an internal promoter within the *pdxA* reading frame (P_{ksgA}; Fig. 1A). It was reported that synthesis of *ksgA* depends on translation coupling to the upstream reading frame, which turned out to be *pdxA* (72, 73). It is unknown how such coupling, if necessary, could be accomplished for transcripts that initiate at P_{ksgA}.

pdxB encodes a pivotal 4-phosphoerythronate dehydroge-

* Corresponding author. Present address: Lilly Research Laboratories, Lilly Corporate Center Drop Code 1543, Indianapolis, IN 46285. Phone: (317) 433-0095. Fax: (317) 276-9159. E-mail: Winkler_Malcolm_E@Lilly.com.

† Present address: Villa Julie College, Stevenson, MD 21153.

‡ Present address: Department of Molecular and Human Genetics, Baylor College of Medicine, Houston, TX 77030.

§ Present address: Lilly Research Laboratories, Indianapolis, IN 46285.

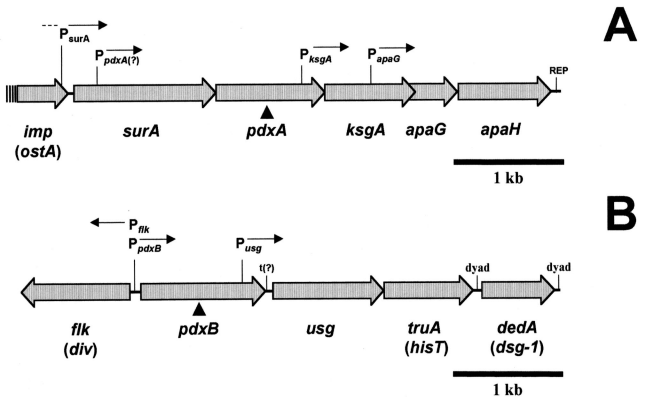

FIG. 1. Structures of the *pdxA* and *pdxB* superoperons. (A) *pdxA* superoperon. The site of insertion of the *pdxA*::mini-MudI *lacZ* element in strain NU1187 (determined by restriction analysis) (55) is indicated by the solid triangle. The product of the *imp* gene is involved in organic solvent tolerance (1), and *surA* encodes a periplasmic peptidyl-prolyl isomerase that assists in the proper folding of outer membrane proteins (42, 57, 66). The likely position of the P_{surA} promoter is indicated (66). The probe for detection of *pdxA-ksgA* cotranscripts and *ksgA*-specific transcripts covers the region between the *Bgl*I and *Pvu*II sites (see Materials and Methods) (55). (B) *pdxB* superoperon. The site of insertion of the *pdxB*::mini-MudII *lacZ* translational fusion element in NU1702 (solid triangle) was determined to be in frame by DNA sequencing (59). The probes for detection of *pdxB* and P_{flk} cover the region between the *Hin*dIII and *Taq*I sites (see Materials and Methods; 59).

nase that is the first enzyme utilized solely by the de novo PLP biosynthetic pathway (40, 77). The *pdxB* gene is the first gene in a complex superoperon that encodes *usg* (paralog of *asd*, which encodes aspartate semialdehyde dehydrogenase), *truA* (*hisT*; encodes tRNA modification enzyme pseudouridine synthase I), and *dsg* (encodes a putative inner membrane protein of unknown function) (Fig. 1B) (2, 3). About half of the amount of *usg-truA-dsg* transcripts originates from an internal promoter located within the *pdxB* coding region (P_{int}; Fig. 1B) in exponentially growing *E. coli* (2, 3). *pdxB* is divergently transcribed from *flk*, which acts as a positive regulator that couples translation of the FlgM regulator to flagellar ring assembly (35, 59). The −10 regions of the P_{pdxB} and P_{flk} promoters overlap; however, no link between *pdxB* and *flk* regulation and functions has been reported (35, 59).

To fully understand the control and integration of PLP biosynthesis, we have been determining whether the individual PLP biosynthetic genes are subject to forms of metabolic regulation. Previously, we reported that the *serC* (*pdxF*) gene is positively regulated by the Lrp protein and negatively regulated by the cyclic AMP receptor protein (43). Here we report that transcription of the *pdxA* and *pdxB* genes is positively growth rate regulated by two different mechanisms. The Fis regulatory protein mediates *pdxA* regulation and part of *ksgA* regulation, whereas *pdxB* is regulated by an unknown mechanism. We also report that *pdxJ* expression is constant with respect to growth rate.

MATERIALS AND METHODS

Bacterial strains and plasmids. The bacterial strains, plasmids, and phages used in this study are listed in Table 1. Markers were moved between strains by generalized transduction with P1 *kc* or P1 *vir* bacteriophage as previously described (46). Recombinant plasmids were constructed by using standard techniques (4). Plasmid clones of the *pdxA* upstream flanking region were derived from Kohara phage clone 8D2 (37), which was provided by K. Rudd. Insertional mutagenesis in plasmids with the mini-MudI (Km^r) and mini-MudII (Km^r) fusion elements was performed as previously described (14). Insertion sites in plasmids were determined by restriction analysis and by DNA sequencing for translational fusions obtained with mini-MudII (Km^r). Plasmids used for double stranded sequencing were prepared by a combined alkaline lysis and polyethylene glycol precipitation method (4). Kanamycin-resistant insertions were crossed from linearized plasmids into the chromosome of *recBC sbc* mutant JC7623 as described previously (3).

Media and culture conditions. *E. coli* strains were grown in Luria-Bertani (LB) medium or minimal 1×E media prepared as previously described (2). Minimal salts-glucose medium contained 1×E salts, 0.01 mM $FeSO_4$, and 0.4% (wt/vol) glucose. α-Methylglucoside was added at a 5:1 ratio to glucose. Minimal salts-glycerol medium (MMGly) contained 0.6% (wt/vol) glycerol, and minimal salts-acetate medium contained 0.6% (wt/vol) potassium acetate. Enriched minimal salts-glucose medium (EMMG), enriched minimal salts-glycerol medium, enriched minimal salts-acetate medium, and enriched minimal salts medium all contained amino acids supplied in the form of 0.5% (wt/vol) vitamin assay Casamino Acids (Difco Laboratories, Detroit, Mich.) plus 0.1 mM L-tryptophan. When indicated, PN was supplemented at 5×10^{-7} M (17). When required, ampicillin and kanamycin were added to LB or minimal media at 50 and 25 μg/ml, respectively, and chloramphenicol was added at 25 and 12.5 μg/ml, respectively.

β-Galactosidase enzyme assays. Strains were grown in different culture media to vary growth rates to cell densities of about 70 Klett units (≈4×10^8 cells/ml) on a Klett-Summerson colorimeter with a number 66 red filter, and cell extracts were prepared for determination of β-galactosidase activity as described previously (46). β-Galactosidase specific activities were expressed as Miller units (46).

RNA isolation and transcript analysis. Bacteria were grown at 37°C with shaking in LB or minimal medium to cell densities of about 70 Klett units, except under the conditions of *relA* overproduction or amino acid starvation (see below). Total cellular RNA isolation and RNase T_2 protection assays for transcript analysis were done as described previously (70). Plasmid template pNU180 was used for synthesis of an RNA probe that detects *pdxA-ksgA* cotranscripts and *ksgA*-specific transcripts (55). This probe covers the region between *Bgl*I and *Pvu*II shown in Fig. 1A. pNU200 was used for the *pdxB* and P_{flk} probes (59). These probes cover the region between *Hin*dIII and *Taq*I shown in Fig. 1B. The *pdxB* probe was synthesized from linearized plasmid by using SP6 RNA polymerase, and the P_{flk} probe was synthesized from linearized plasmid by using T7 RNA polymerase. All RNA probes were synthesized by using the Riboprobe Gemini system in accordance with the manufacturer's instructions. For RNA preparations used in transcript half-life ($t_{1/2}$) determinations, cells were grown in the indicated medium and rifampin was added to a final concentration of 0.5 mg/ml. Samples were taken immediately prior to rifampin addition ($t = 0$) and from 2 to 10 min after addition of the drug. Transcript analysis was performed on each sample, and $t_{1/2}$s of mRNAs were calculated from the slope of a least-squares regression line of the amount of RNA remaining plotted semilogarithmically against time after rifampin addition.

Amino acid starvation. *E. coli* prototroph strain NU426 or NU816 and strain TX1892 (NU426 Δ*relA*) (Table 1) were grown in LB medium supplemented with 0.4% (wt/vol) glucose (LB-Glc) at 37°C to an optical density at 420 nm of 0.65 (15). Amino acid starvation was induced by the addition of 1 mg of serine hydroxymate per ml, which competitively inhibits seryl-tRNA synthetase and provokes the stringent response in wild-type *E. coli* (15). Samples for transcript analysis were taken 20 min after serine hydroxymate addition (15).

RelA overexpression. TX2737 carrying pALS13 was used to overexpress the RelA protein, and TX2739 (Table 1) was used as a control. pALS13 encodes a truncated form of *relA* (the first 455 of the 743 amino acids of RelA) under the control of the isopropyl-β-D-thiogalactopyranoside (IPTG)-inducible P_{tac} promoter. The truncated form of RelA is functional for guanosine tetraphosphate (ppGpp) synthesis independent of ribosomes (60, 64). pALS14, which encodes a form of RelA that is more truncated (331 amino acids) and is not functional for ppGpp synthesis, served as a control. Cells were grown to an optical density at 600 nm of 0.4 in glucose minimal medium supplemented with 0.5% amino acids, and RelA expression was induced with 100 μM IPTG. Samples for transcript analysis were taken immediately prior to IPTG addition and 20 min following IPTG addition.

Normalization of growth rate-regulated parameters. Specific activities were converted to rate of enzyme accumulation per genome in accordance with the equation of Tribe et al. (68), $q = \mu \ln 2/60 \times S \times P/G$, where P/G is the amount

TABLE 1. Bacterial strains and plasmids used in this study

Strain or plasmid	Genotype[a]	Source or reference
Strains		
AL0875	*thi-1 leu6 lacY1 lacIZ* Δ*(mlu) supE44 tonA21 rpsL rfbD1 lipB*::mini-Tn*10*	54
CAG12093	MG1655 *car-96*::Tn*10*	62
CF1693	MG1655 Δ*relA251*::*kan* Δ*spoT207*::*cat*; Cm^r Km^r	M. Cashel collection
JC7623	*arg ara his leu pro recB21 recC22 sbcB15 thr*	55
RJ1529	MG1655 *fis*::*767* Δ*(lac-pro) ara str*	5
NK7049	Δ*lacX74 galOP308 rpsL* Sm^r	61
NU426	W3110 prototroph	C. Yanofsky collection
NU816	Single colony isolate of W3110 *tnaA2* Δ*lacU169*	C. Yanofsky collection
NU1187	NU816 *pdxA*::mini-Mud-1-1 Km^r	55
NU1700	JC7623 *pdxB*::mini-MudII Km^r	Transformation with linearized pNU250; this study
NU1702	NU816 *pdxB*::mini-MudII Km^r	NU816 × P1 *kc* NU1700
TX1892	NU816 Δ*relA251*::*kan*; Km^r	NU816 × P1 *kc* (CF1693) This study
TX2093	NU1187(pNO2661, pNO2696)	This study
TX2094	NU1187(pNO1301)	This study
TX2095	NU1187(pNO1302)	This study
TX2096	NU1187(pBR322)	This study
TX2169	NU1187(pNU122)	This study
TX2171	NU1187(pUC19)	This study
TX2243	NU1187(pBR322, pACYC184)	This study
TX2254	NU1187(pNU276)	This study
TX2269	NU1187(pPR274)	This study
TX2283	NU1702(pTX291)	This study
TX2357	NU1187(pTX288)	This study
TX2737	NU426(pALS13)	This study
TX2739	NU426(pALS14)	This study
TX3333	NU426 *fis*::*767*	NU426 × P1 *vir* (RJ1529)
TX3338	NU426 *lipB*::mini-Tn*10*; Tc^r	NU426 × P1 *vir* (AL0875)
TX4080	NK7049 with *pdxJ-lacZ* protein fusion λRS641; Sm^r	This study
TX4082	NK7049 with *pdxJ-lacZ* protein fusion λRS643; Sm^r	This study
Plasmids		
pACYC184	Replicon P15A; Cm^r Tc^r	46
pALS13	P_{tac}::*relA′* (445 N-terminal amino acids of *relA*) *lacI*^{q}	64
pALS14	P_{tac}::*relA′* (331 N-terminal amino acids of *relA*) *lacI*^{q}, Ap^r	64
pBR322	Replicon ColE1; Ap^r Tc^r	46
pGEM3Z	pUC18 derivative with phage T7 and SP6 promoters	Promega
pNO1301	pBR322 (*rrnB*$^+$); Ap^r	33
pNO1302	pNO1301 with 2.45-kb deletion in *rrnB*; Ap^r	33
pNO2661	pACYC184 (RNA polymerase β and β′) Cm^r	8
pNO2696	pBR322 (RNA polymerase α and σ^{70}) Ap^r	8
pNU122	pUC19 (*pdxA*$^+$ *ksgA*$^+$ *apaG*$^+$ *apaH*$^+$); Ap^r	55
pNU180	pGEM3Z (386-bp *pdxA-ksgA* region); Ap^r	59
pPR274	mini-F′ replicon; Cm^r *trpE*$^+$	47
pNU276	pBR322 (*pdxA*$^+$ plus upstream region) 5.0-kb *Eco*RI fragment from Kohara phage clone 8D2; Ap^r	This study
pTX288	pPR274 (*pdxA*$^+$) same insert as plasmid pNU276; Cm^r	This study
pTX291	pPR274 (*pdxB*$^+$) 4.4-kb insert containing entire *pdxB* operon; Cm^r	This study
Phage λ-borne *lacZ* fusions		
λRS641	Δ*rnc-36 era*$^+$ *recO*$^+$ *pdxJ′*::*lacZ′*	45
λRS643	Δ*rnc-76* Δ*rnc-36 era*$^+$ *recO*$^+$ *pdxJ′*::*′lacZ*	45

[a] Ap^r, Cm^r, Km^r, and Tc^r indicate resistance to ampicillin, chloramphenicol, kanamycin, and tetracycline, respectively.

of protein per genome, extrapolated from the data of Bremer and Dennis (10), and S is specific activity. The term $\mu \ln 2/60 \times S$ is equivalent to dP/dt (10), so q is equivalent to the instantaneous rate of accumulation of a protein normalized to the total DNA of the *E. coli* genome. To relate q to the relative gene frequency with respect to μ, F_g was first calculated as follows: $F_g = c\ln 2/60 \times \mu \times 2^{(c)(\mu/60)(1-x)} \times 1/2^{(c)(\mu/60)} - 1$, where c is 45 min, which is the transit time for the chromosome replication fork (10), and x is the relative distance of the particular gene from the replication origin. q_g was then calculated as follows: $q_g = q/F_g \times 4.22 \times 10^{-2}$ mg. The amount of a given mRNA is related to gene frequency as follows: r = amount of specific mRNA/$R \times R/G$, where R is the total amount of RNA and R/G is the total amount of RNA per genome, extrapolated from the data of Bremer and Dennis (10). Then, $r_g = r/F_g \times 4.22 \times 10^{-2}$ mg.

RESULTS

Growth rate-regulated expression of *lacZ* fusions to *pdxA* and *pdxB*. To analyze the regulation of *pdxA* and *pdxB*, we constructed *lacZ* fusions in *pdxA* and *pdxB* at their native

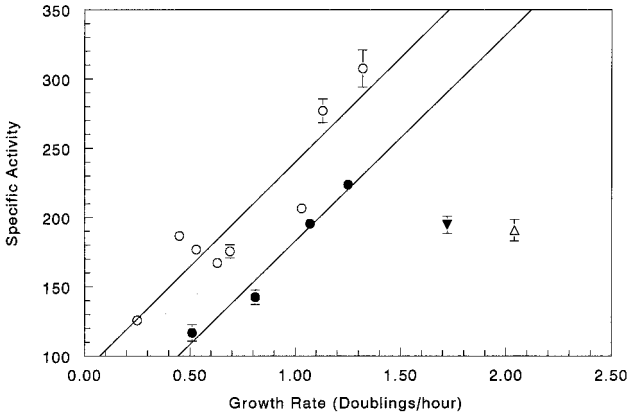

FIG. 2. Growth rate regulation of *pdxA*- and *pdxB-lacZ* fusions in strains NU1187 (open symbols) and NU1702 (closed symbols), respectively. Cells were grown exponentially in minimal media containing different carbon sources (circles) or in LB (triangles) (see Materials and Methods). Specific activities of β-galactosidase were determined (see Materials and Methods) and plotted as a function of the growth rate expressed as doublings per hour (μ). The results shown are from at least three independent cultures at each growth rate. The error bars represent the standard error of the mean. Lack of error bars indicates that the standard error of the mean was negligible.

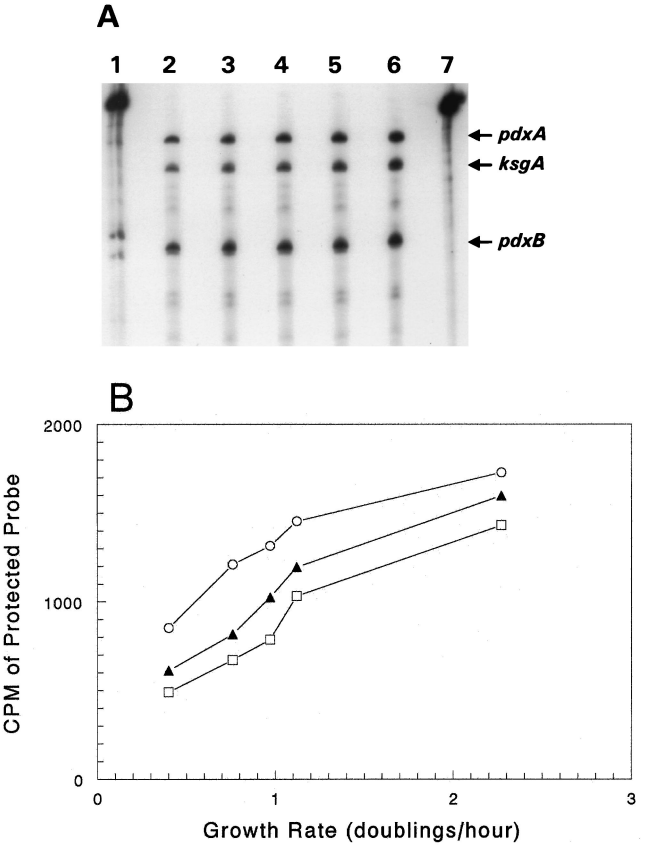

FIG. 3. Amounts of *pdxA-ksgA* cotranscript and *ksgA*- and *pdxB*-specific transcripts in exponentially growing *E. coli* K-12. (A) Autoradiograph of RNase T_2 protection assays. Equal amounts (50 μg) of RNA prepared from cultures of prototrophic strain NU426 grown in MMGly (lane 2), minimal salts-glucose medium (lane 3), enriched minimal salts-glycerol medium (lane 4), EMMG (lane 5), and LB (lane 6) were probed as described in Materials and Methods. Positions of bands corresponding to the *pdxA-ksgA* cotranscript (labeled *pdxA*) and the *ksgA*- and *pdxB*-specific transcripts are indicated. Lanes 1 and 7 show the undigested *pdxA-ksgA* and *pdxB* probes, respectively. The results were from at least three independent cultures at each growth rate. (B) Counts per minute corresponding to the *pdxA-ksgA* cotranscript (filled triangles), the *ksgA*-specific transcript (open rectangles), and the *pdxB*-specific transcript (open circles) were determined from gels such as the one in panel A by direct counting and plotted as a function of the growth rate.

chromosomal positions in a prototrophic Δ*lac* strain of *E. coli* K-12. Strains NU1187 (55) and NU1702 contain a *pdxA*::mini-MudI *lacZ* transcriptional fusion and a *pdxB*::mini-MudII *lacZ* translational fusion, respectively, at the positions indicated in Fig. 1. We grew strains NU1187 and NU1702 in different media to analyze the expression of *pdxA* or *pdxB* in relation to the cellular growth rate. The corresponding β-galactosidase specific activities under these growth conditions were determined (Fig. 2). The expression of the *pdxA* and *pdxB* genes, as measured by *lacZ* fusions, increased in direct proportion to the growth rate up to 1.3 doublings per hour. The specific activities from the *pdxB-lacZ* translational fusion and, to a lesser extent, the *pdxA-lacZ* transcriptional fusion exhibited an apparent repression when cells were grown in rich LB medium, which supported a growth rate of approximately two doublings per hour (Fig. 2). This apparent reduction disappeared upon normalization (see below).

To find out how common positive growth rate regulation is among genes involved in PLP biosynthesis, we determined the response of *pdxJ* expression to growth rate changes. *pdxJ* is in a complex superoperon that includes the following (in order): *rnc*, *era*, *recO*, *pdxJ*, and *acpS* (41, 65). The major promoter for the operon is before the *rnc* gene (P_{rnc}) with a minor promoter (P_{pdxJ}) for *pdxJ* and *acpS* located at the distal end of *recO* (45). Matsunaga et al. (45) constructed *pdxJ-lacZ* protein fusions expressed from both P_{rnc} and P_{pdxJ} (strain TX4080) or from P_{pdxJ} alone (strain TX4082), integrated into the *E. coli* chromosome at *att*λ. β-Galactosidase specific activities from strain TX4080 or TX4082 were constant within experimental error (scatter between 72 and 103 or 51 and 79 Miller units, respectively) over the eightfold range of growth rates between enriched minimal salts-acetate medium and LB (data not shown). These results were from at least three independent cultures grown in each of the media tested. Thus, we could not detect positive regulation of *pdxJ* expression with increasing growth rate.

Growth rate regulation of *pdxA*, *ksgA*, and *pdxB* transcript amounts. We performed RNase T_2 transcript protection assays (70) to determine whether the observed changes in fusion-specific activities were matched by corresponding changes in *pdxA* and *pdxB* transcript amounts in cells grown at different rates. Equal amounts of total RNA from cells grown at different rates were probed for *pdxA* and *pdxB* transcripts, and the steady-state amounts of *pdxA* and *pdxB* mRNAs were compared. The probe used to detect *pdxA-ksgA* cotranscripts spans the 3′ portion of *pdxA* gene and the 5′ portion of the downstream *ksgA* gene and results in a 386-nucleotide (nt) full-length protected band (Fig. 1A and 3). The probe also detects a shorter protected band of 339 nt that corresponds to *ksgA*-

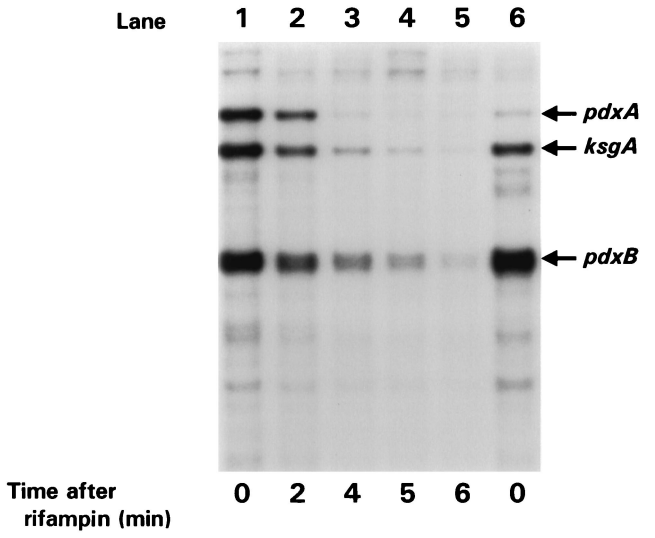

FIG. 4. Determination of the $t_{1/2}$s of the *pdxA-ksgA* cotranscript and *ksgA*- and *pdxB*-specific transcripts of *E. coli* K-12 growing exponentially in LB-Glc. Equal amounts of RNA isolated from NU426 growing in LB-Glc before (lane 1) and at various times after (lanes 2 to 5) rifampin addition were probed as described in Materials and Methods. Positions of bands corresponding to the *pdxA-ksgA* cotranscript and the *ksgA*- and *pdxB*-specific transcripts are indicated. Analogous experiments were performed for NU426 grown at additional growth rates (data not shown; Results). Lane 6, amounts of the same transcripts from NU426 subjected to starvation for amino acids (Results). The results shown are from at least three independent cultures at each growth rate.

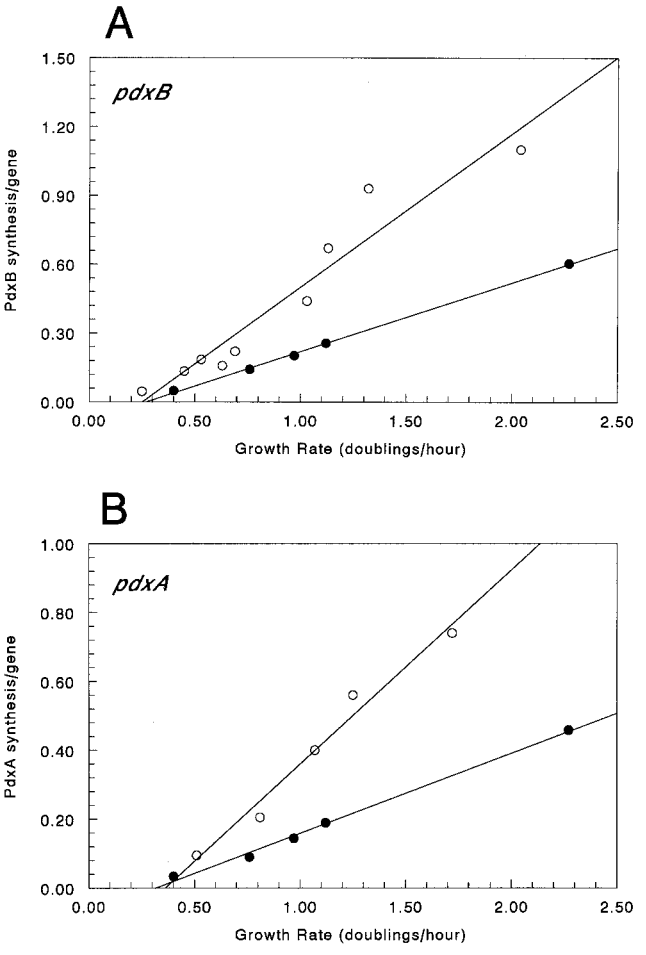

FIG. 5. pdxA and *pdxB* gene expression normalized per gene. The data from Fig. 2 was expressed as rates of protein accumulation per gene (open circles) (see Materials and Methods). The data from Fig. 3B was expressed as the amount of mRNA per gene (closed circles) (see Materials and Methods). Panels: A, *pdxB* gene expression normalized per gene; B, *pdxA* gene expression normalized per gene.

specific transcripts that arise from the *ksgA* internal promoter (P_{ksgA}; Fig. 1A) (55). The *pdxB* probe covers the promoter and transcription start of *pdxB* and results in a single 252-nt protected band (Fig. 1B and 3) (59). A representative experiment showing quantitation of steady-state transcript amounts is shown in Fig. 3B. The amounts of the *pdxA-ksgA* cotranscript and *ksgA*- and *pdxB*-specific transcripts increased relative to the RNA amount in direct proportion to the growth rate, except at the highest growth rate in rich LB medium (Fig. 3B).

The changes in the amounts of steady-state *pdxA-ksgA* cotranscript and *ksgA*-specific and *pdxB*-specific transcripts at different growth rates could reflect changes in transcript stability, as has been demonstrated for the *ompA* and *cat* transcripts (50). Therefore, we analyzed the $t_{1/2}$s of the *pdxA-ksgA* cotranscript and *ksgA*-specific and *pdxB*-specific transcripts with RNase T_2 protection assays by using RNA prepared after rifampin addition to cultures grown at four different growth rates. Figure 4 shows a representative experiment with LB-Glc medium. The *pdxB*-specific and *ksgA*-specific transcripts exhibited a typical pattern for *E. coli* mRNAs of rapid exponential decay (Fig. 4). The stability of the *pdxB*-specific ($t_{1/2} \approx 1.1$ min) and *ksgA*-specific ($t_{1/2} \approx 0.6$ min) transcripts did not vary with the growth rate (data not shown). Thus, growth rate-dependent regulation of *pdxB* and *ksgA* expression is likely to occur at the level of transcription initiation. We could not reach a conclusion for the *pdxA-ksgA* cotranscript because it was extremely unstable. Between 2 and 4 min after rifampin addition, the amount of the *pdxA-ksgA* transcript became undetectable and growth rate-dependent variations in the stability of the short-lived *pdxA* message may not have been detected.

Normalization of gene expression. We wanted to compare and reconcile the determinations obtained for gene fusions and direct transcript amounts. Since a given amount of mRNA can be repeatedly translated, it is not meaningful simply to compare the amounts of transcripts and proteins present in exponentially growing cells (10, 68). Therefore, we applied a method of normalization (see Materials and Methods) to determine the amount of mRNA synthesized per gene and the rate of protein synthesis per gene in bacteria growing at different rates.

There is no simple assay for the activity the PdxB enzyme, so we relied on the β-galactosidase specific activities of a *pdxB-lacZ* translation fusion to reflect the PdxB level. We first assumed that transcription of the *pdxB-lacZ* fusion is the primary target for growth rate regulation. We normalized the specific activities from the *pdxB-lacZ* fusion and the amount of the *pdxB*-specific transcript on a per-gene basis in accordance with the equations of Tribe et al. (68) in order to compare the data

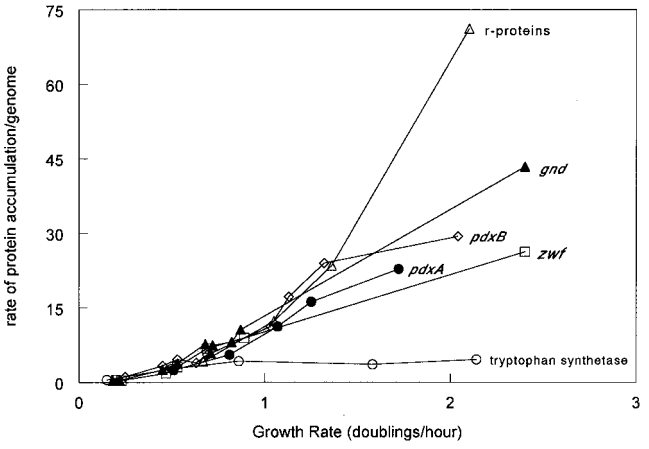

FIG. 6. Rate of accumulation of several proteins normalized per genome (see Materials and Methods) plotted as a function of the growth rate (μ) in doublings per hour. Symbols: PdxB, open triangles; r-proteins, open triangles; tryptophan synthetase (TrpAB), open circles; PdxA, filled circles; Gnd, filled triangles; Zwf, open rectangles.

in Fig. 2 and 3 directly. As shown in Fig. 5A, the curve for the rate of enzyme accumulation per gene for the *pdxB-lacZ* fusion is about twofold steeper than that of the corresponding curve for the amount of *pdxB* mRNA synthesized per gene. This difference corresponds to and likely reflects the increase in the overall translational efficiency with increasing growth rate over the growth rates used in these experiments (10).

A similar analysis was performed for *pdxA*. In this case, a *pdxA-lacZ* transcription fusion was assayed, so this analysis tested whether expression of the *pdxA-lacZ* fusion was truly correlated with *pdxA* transcript accumulation. Similar to the case for *pdxB*, the curve for the rate of amount of enzyme accumulation per gene for the *pdxA-lacZ* fusion is about twofold steeper than that of the corresponding curve for the amount of *pdxA* mRNA synthesized per gene (Fig. 5B).

Figure 2 shows that the β-galactosidase specific activities encoded by the *pdxB-lacZ* and *pdxA-lacZ* fusions apparently failed to keep up with the growth rate change at the highest growth rate. When normalized on a per-gene basis, expression of both the *pdxB* and *pdxA* genes is proportional to the growth rate at all of the growth rates tested (Fig. 5). Thus, the apparent repression at the highest growth rate (Fig. 2) disappeared following normalization (Fig. 5).

We compared the normalized growth rate regulation of *pdxA* and *pdxB* with that of other genes that have been reported to be growth rate regulated. For the following proteins, we used the data in the references cited to calculate the accumulation rate per genome (see Materials and Methods), which was plotted against the growth rate (μ) (Fig. 6) on the basis of the references cited: ribosomal protein (r-protein) gene expression (20), PdxB (from β-galactosidase activity of a translational fusion [Fig. 5A]), PdxA (from β-galactosidase activity of a transcriptional fusion [Fig. 5B]), 6-phosphogluconate (6PGD; encoded by *gnd*) (75), glucose 6-phosphate dehydrogenase (G6PD, encoded by *zwf*) (75), and tryptophan synthetase (56). The r-protein genes (20) and metabolic enzymes are found at several locations in the *E. coli* chromosome. Therefore, all expression was normalized on a per-genome basis, which gave only slightly different results from normalization on a per-gene basis. For example, the term F_g varies from 1.09 to 1.3 for $\mu = 0.5$ to 1.7 for *pdxA* expression, whereas F_g is virtually invariant for *pdxB* over an even wider range of growth rates.

Normalization shows that growth rate regulation of *pdxA*, *pdxB*, *gnd*, and *zwf* (Fig. 6) extends over a much larger range of growth rates than is apparent from a simple comparison of enzyme specific activities (Fig. 2) (75). In cells grown in LB medium, the specific activities of *pdxA*, *pdxB*, *gnd*, and *zwf* apparently decrease compared to the specific activities from cells grown in glucose minimal medium (Fig. 2) (75). When normalized on a per-genome basis, *pdxA*, *pdxB*, *gnd*, and *zwf* gene expression is proportional to the growth rate at all of the growth rates tested (Fig. 6). Thus, the apparent repression at the highest growth rates (Fig. 2) (75) disappears following normalization (Fig. 6). Growth rate regulation of the r-protein genes is even greater than that of *pdxA*, *pdxB*, *gnd*, and *zwf* (Fig. 6). Tryptophan synthetase is far less affected by the growth rate than are *pdxA*, *pdxB*, *gnd*, and *zwf* (Fig. 6).

A *fis* mutation abolished the growth rate regulation of *pdxA-ksgA* but not that of *pdxB*. We tested the effect of a null mutation in the *fis* gene on the growth rate-dependent regulation of *pdxA* and *pdxB*. The Δ*fis-767*::*kan* allele (34) was transduced into NU426 by P1 transduction. The resulting strain, TX3333, had similar growth rates in three different minimal media, including acetate, glycerol, and glucose plus amino acids compared to that of NU426 (Fig. 7). The increase in the amount of *pdxA-ksgA* cotranscript as a fraction of the total RNA from TX3333 cells was only 25% of that seen in the *fis*$^+$ parent strain as a function of the growth rate (Fig. 7A). In contrast, the increase, along with that of the growth rate, of the amounts of *ksgA*- and *pdxB*-specific transcripts was the same in the *fis*$^+$ parent and *fis* mutant cells (Fig. 7B and D). Thus, only about half of the total amount of the *ksgA* transcript was subject to control by *fis* (Fig. 7C).

ppGpp concentrations influence *pdxA* and *ksgA*, but not *pdxB*, transcript amounts. We tested the effect of high levels of ppGpp on *pdxA*, *ksgA*, and *pdxB* expression by inducing the stringent response. We determined the amounts of the *pdxA-ksgA* cotranscript and *ksgA*- and *pdxB*-specific transcripts in *relA*$^+$ (NU426) and Δ*relA251* (TX1892) strains grown in LB-Glc medium before and after amino acid starvation induced by the addition of 1 mg of serine hydroxymate per ml (15). The *relA* gene is necessary for the stringent control of rRNA (reviewed in reference 13).

A representative experiment comparing transcript levels is shown in Fig. 4 (lanes 1 and 6), and results from several experiments are averaged in Table 2. The amount of the *pdxB*-specific transcript was unaffected by amino acid starvation (Table 2). In contrast, the *pdxA-ksgA* cotranscript or *ksgA*-specific transcript amount was strongly (6-fold) or moderately (≈1.5-fold) decreased, respectively, during amino acid starvation in the *relA*$^+$ parent strain. The decrease in the *pdxA-ksgA* cotranscript or *ksgA*-specific transcript amount was independent of or dependent on *relA* function, respectively (Table 2). The *relA*-independent decrease in the amount of the *pdxA-ksgA* cotranscript may simply reflect the decrease in the growth rate caused by amino acid limitation (Fig. 2 to 5) and was not examined further. The net effect of this regulatory pattern on the total

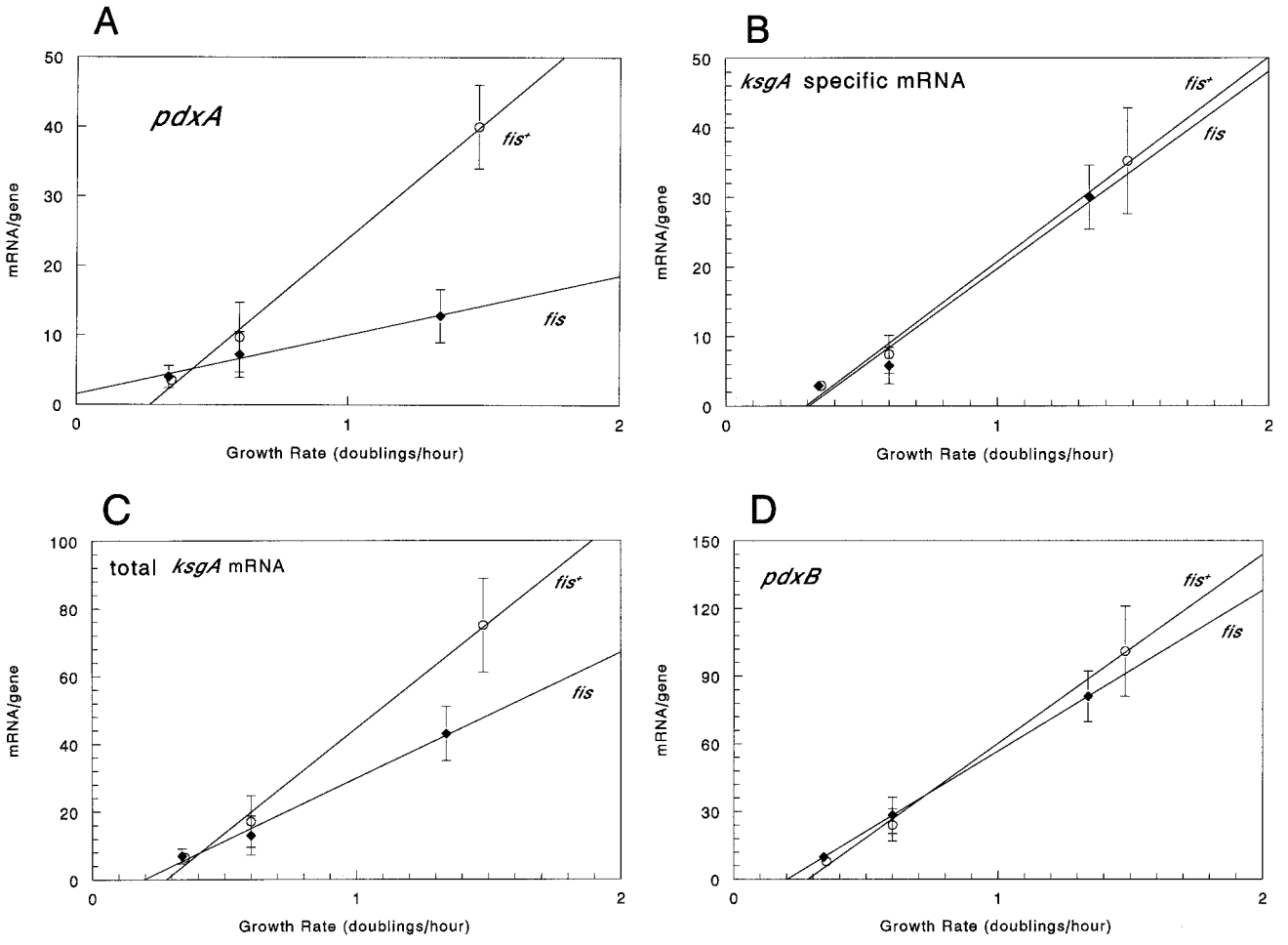

FIG. 7. Effect of a *fis* mutation on the growth rate regulation of the amount of the *pdxA-ksgA* cotranscript, the amount of the *ksgA*- and *pdxB*-specific transcripts, and the total amount of the *ksgA* transcript. Total RNA isolated from NU426 (open symbols) or TX3333 (NU426 *fis*) (closed symbols) growing exponentially in minimal salts-acetate medium, MMGly, or EMMG was probed as described in Materials and Methods. Counts per minute corresponding to individual bands were expressed as the amount of mRNA per gene (see Materials and Methods), and the average amount of mRNA per gene for each transcript was calculated from three and four independent experiments for NU426 and TX3333, respectively, and plotted against the growth rate. Standard deviations of the mean are shown. Panels: A, *pdxA-ksgA* cotranscript; B, *ksgA*-specific transcript; C, total *ksgA* transcript (sum of panels A and B); D, *pdxB*-specific transcript.

ksgA transcript amount is a moderate stringent response of about 2.3-fold (Table 2).

We attempted to determine the effect of amino acid starvation on transcript $t_{1/2}$s. However, we found that there was a marked lag after rifampin addition before decay of the transcripts became apparent (data not shown). This lag varied in length between experiments; consequently, transcript $t_{1/2}$s could not be determined reliably following amino acid starvation. The permeability of *E. coli* cells to many molecules is altered during amino acid starvation (13), and it seems possible that amino acid starvation induced by serine hydroxymate decreases the permeability of *E. coli* for rifampin.

We also mimicked induction of the stringent response by overproducing the RelA protein under the control of the P_{tac} promoter in strain NU426 (pALS13 and pALS14, Table 1; data not shown; 60, 64). Addition of 100 μM IPTG has been shown to cause rapid accumulation of ppGpp in analogous strains approximately to the level detected during the stringent response (60, 64). Induction of RelA overexpression quickly inhibits the growth rate (60), which we observed for strain NU426 (data not shown). When RelA was overexpressed, the amounts of the *pdxA-ksgA* cotranscript and *ksgA*- and *pdxB*-specific transcripts changed in ways similar to those seen during amino-acid starvation (data not shown; Table 2).

RelA overexpression extended the $t_{1/2}$s of the *ksgA*-specific transcript ($t_{1/2} \approx 1.2$ min instead of 0.6 min) and the *pdxA-ksgA* cotranscript so that it could be determined ($t_{1/2} \approx 1.4$ min). In contrast, the $t_{1/2}$ of the *pdxB*-specific transcript remained about 1.1 min following RelA overexpression. In this experiment, transcript decay curves appeared normal and did not contain lags (data not shown). Thus, the *relA*-independent decrease in the *pdxA-ksgA* transcript amount may involve decreased transcription initiation that is partially offset by increased transcript stability. On the other hand, we cannot rule out complex differential effects of rifampin uptake that would affect the quantitation of the *pdxA-ksgA* cotranscript differently from that of the *pdxB*-specific transcript.

Other putative effectors did not influence *pdxA* and *pdxB*

TABLE 2. Relative changes in transcript amounts of the *pdxB*-, *flk*-, and *ksgA*-specific transcripts and the *pdxA-ksgA* cotranscript in exponentially growing and amino acid-starved *E. coli* K-12

Transcript[a]	Ratio of transcript amounts (unstarved/amino acid starved)[b]	
	relA$^+$ parent strain[c]	Δ*relA* mutant[d]
pdxB specific	0.8 ± 0.1	0.8 ± 0.2
flk specific	1.7 ± 0.4	1.0 ± 0.5
pdxA-ksgA cotranscript	5.9 ± 0.8	6.6 ± 1.7
ksgA specific	1.6 ± 0.2	0.6 ± 0.1
Total *ksgA*	2.3 ± 0.3	0.8 ± 0.1

[a] See Fig. 1 and the text for the locations and functions of genes.
[b] Cells were grown in LB medium supplemented with 0.4% glucose at 37°C to an OD_{420} of 0.65 with shaking. Amino acid starvation was caused by addition of 1 mg of serine hydroxymate per ml (see Materials and Methods) (67). Samples for RNase T_2 protection assays were taken immediately prior to serine hydroxymate addition (unstarved) and 20 min after serine hydroxymate addition (amino acid starved) (see Materials and Methods). Means with standard errors were obtained from several independent experiments
[c] The *relA*$^+$ strain was either NU426 or NU816 (Table 1), which gave similar results.
[d] The Δ*relA* strain was NU1892 (NU816 Δ*relA251*) (Table 1).

growth rate regulation. We tested several other putative effectors of growth rate regulation to learn whether they influence *pdxA* and *pdxB* expression. *lipB* was proposed as a negative effector of the growth rate regulation of the *dam* gene (71). *lipB* encodes a lipoyltransferase that transfers endogenously synthesized lipoate to apoproteins (49). However, a *lipB* null mutation did not influence the amounts or growth rate regulation of the *pdxA-ksgA* cotranscript or the *ksgA*- and *pdxB*-specific transcripts (Table 1; data not shown). We tested whether RNA polymerase is limiting within the cell, resulting in some form of promoter competition (32). However, the growth rate regulation of the *pdxA-lacZ* fusion (Fig. 2) was not affected by plasmids (pNO2661 and pNO2096) expressing extra copies of the α, β, β′, and σ^{70} subunits or RNA polymerase (Table 1; data not shown; 8). Similarly, growth rate regulation of the *pdxA-lacZ* fusion was not affected by the presence of a plasmid (pNO1301) containing the highly expressed *rrnB* operon (Table 1; data not shown).

Finally, we were unable to detect autoregulation of *pdxA* or regulation of *pdxA* or *pdxB* in response to added B_6 vitamers such as PN. In these experiments, the *pdxA*$^+$ gene, including the upstream promoter region, was cloned into a single-copy mini-F′ vector (pTX288) or multicopy vectors (pNU122 and pNU276; Table 1). Transformation of these plasmids into the corresponding *pdxA-lacZ* (NU1187) chromosomal fusion strain resulted in prototrophy for PN (data not shown). Expression of *pdxA*$^+$ from single-copy or multicopy plasmids did not significantly affect the expression level or the growth rate regulation of the *pdxA-lacZ* fusion (data not shown). In an analogous experiment, *pdxB*$^+$ cloned into a single-copy mini F′ vector (pTX291, Table 1) did not affect the expression or growth rate regulation of the *pdxB-lacZ* fusion NU1702 (data not shown). Addition of exogenous PN to 5×10^{-5} M, which was about 100-fold more than that required to support the full growth of auxotrophs, did not affect the expression of the *pdxA*- or *pdxB-lacZ* fusion (data not shown).

DISCUSSION

We report here that expression of the *pdxA*, *ksgA*, and *pdxB* genes is strongly regulated by cellular growth rate changes (Fig. 2 and 3). Expression of PdxA and PdxB normalized as the rate of accumulation per gene increased 6-fold and 20-fold over 2.5- and 5-fold ranges of increasing growth rates, respectively (Fig. 5). The levels of all *E. coli* proteins are coordinated in some way with the cellular growth rate. With two-dimensional gel electrophoresis, it was demonstrated that three basic patterns describe the relationship between the cellular growth rate and the relative amount of individual proteins (52). One pattern includes proteins that increase with growth rate increases over a wide range of growth rates, and PdxA and PdxB are within this class. As a fraction of the total protein, these proteins increase proportionately as the growth rate increases. The total amount of protein per cell itself increases as the growth rate increases (10). Thus, if the level of a protein increases as a fraction of the total protein with an increase in the growth rate, the absolute rate of accumulation of that protein is equal to at least the square of the increase in the growth rate. As a fraction of the total protein, both PdxA and PdxB increased when the growth rate increased (Fig. 2) and the absolute rate of accumulation per gene of both PdxA and PdxB increased well beyond the increase in the growth rate (Fig. 5). Other proteins in this class comprise a large fraction of the cellular bulk protein and include proteins involved in translation, such as r-proteins, tRNA synthetases, and elongation factors. The fraction of the total protein of those proteins varied from 20 to 55% over a fivefold range of growth rates. When we normalized these r-proteins as the absolute rate of accumulation per genome, we noticed that the rate of accumulation of these proteins was actually more than the square of the increase in the growth rate (Fig. 6). The amounts of rRNA and most tRNAs are also positively regulated over a wide range of growth rates (10).

The change in the rate of accumulation of the PdxA- and PdxB-LacZ fusion proteins per gene was greater than the change in *pdxA* and *pdxB* transcript amounts with changes in the growth rate (Fig. 5). This result is consistent with an increase in the overall cellular translational efficiency with an increase in the growth rate (10). Thus, the *pdxA* and *pdxB* transcripts seem to take advantage of the increased ribosome capacity that accompanies a growth rate increase.

We observed that the specific activity of β-galactosidase from the *pdxA*- and *pdxB-lacZ* fusions decreased at the highest growth rate in rich LB medium (Fig. 2). A similar pattern of apparent repression had been reported for 6PGD (Zwf), G6PD (Gnd) (75), and tryptophan synthetase (TrpAB) and was referred to as metabolic regulation (56). However, when normalized, the rates of accumulation of 6PGD, G6PD, PdxA, and PdxB per genome all still increase proportionally with the growth rate (μ) in rich media, whereas that of TrpAB levels off. Thus, normalization analysis revealed differences in gene expression with growth rate between the *trp* operon genes and the other genes described above that were not apparent by simply comparing the specific activities at different growth rates.

We attempted to find mechanisms that underlie the growth rate regulation of *pdxA*, *ksgA*, and *pdxB*. We found that growth

rate regulation of the amount of *pdxA-ksgA* cotranscript, but not that of the *pdxB*- and *ksgA*-specific transcripts, was mediated by the Fis protein (Fig. 7). Fis is a small, basic, nucleoid-associated protein that functions as a dimer and binds to and bends DNA (25). Fis mediates a wide range of cellular processes, including site-specific recombination, positive and negative regulation of the transcription of many protein-encoding genes, and growth rate regulation of stable RNA genes (25, 76). Fis-dependent activation of *rrn* operons is not growth rate dependent and appears to be dispensable (6). However, under special circumstances, Fis can become the growth rate-dependent regulator of *rrn* operons (7). Fis mediates the positive growth rate regulation of 4.5S RNA but not that of M1 RNA (22). Fis positively and negatively regulates different tRNA operons with growth rate (24, 58).

The positive regulation of the *pdxA-ksgA* cotranscript amount by Fis with growth rate (Fig. 7) resembles that of tRNA operons (24, 58). We do know whether this regulation is direct or indirect. The promoter(s) for *pdxA* is located somewhere upstream of *pdxA* (Fig. 1A) (55). *surA* is located immediately upstream and overlaps *pdxA* (Fig. 1A) (66). The P_{surA} promoter, which must drive the formation of a *surA-pdxA-ksgA* cotranscript, has been preliminarily mapped to the end of *imp* (Fig. 1A), which immediately precedes *surA* and is involved in tolerance to organic solvents (1). Preliminary experiments indicate that transcription of the *pdxA-ksgA* cotranscript may also originate at a second promoter located in the 5′ end of *surA* upstream from the insertion mutations in *surA* that are polar on *pdxA* expression and cause PN auxotrophy 66; Kolter, personal communication). The DNA sequence in the vicinity of the putative P_{surA} promoter contains several potential Fis binding sites (data not shown) (25). Whether these sites play a role in Fis-dependent growth rate regulation of the *pdxA-ksgA* cotranscript will be determined in future experiments.

We tested the effects of several other potential regulators of growth rate regulation on *pdxA* and *pdxB* expression. The amounts of the *pdxA-ksgA*- and *pdxB*-specific transcripts were not regulated by a ppGpp-mediated stringent response, although the amount of the *pdxA-ksgA* cotranscript was significantly decreased by conditions that limited bacterial growth (Table 2; Results). We did detect a modest level of stringent regulation of *ksgA*-specific and total *ksgA* transcript amounts (Table 2). Autoregulation of *pdxA* or *pdxB* expression was not detected, and *pdxA* and *pdxB* expression did not respond to the amount of B_6 vitamer added to growth media or to starvation for B_6 vitamers (Results; data not shown). We did not detect effects of a *lipB* mutation, overexpression of RNA polymerase subunits, or the presence of strong *rrnB* promoters on *pdxA* expression (Results). Thus, the growth rate regulation of the *pdxA-ksgA* cotranscript amount was directly or indirectly mediated by Fis whereas the mechanism of growth rate regulation of *pdxB* remains unknown.

It was recently reported that the concentration of the initiating nucleotide triphosphate may determine the growth rate regulation of *rrn* promoters (27), although this regulation may be more complicated than it first appeared (53). *pdxA* and *pdxB* expression is unlikely to be affected by the concentration of initiating nucleoside triphosphates because only strong promoters with short-lived complexes with RNA polymerase are affected by the initiating nucleoside triphosphate concentration (27). Moreover, the *pdxB* promoter does not contain any of the elements common to rRNA promoters and tRNA promoters, such as the GC-rich discriminator region that is necessary for the regulation of those promoters (27). Consequently, we did not test the effect of the cellular nucleotide concentration on *pdxA* and *pdxB* growth rate regulation.

Our present level of knowledge is not sufficient to predict what role, if any, the strong growth rate regulation of *pdxA* and *pdxB* (Fig. 7) has in the flux of intermediates through the de novo pathway of PLP biosynthesis. Moreover, other PLP biosynthetic genes do not follow the pattern of positive growth rate regulation reported here for *pdxA* and *pdxB*. For example, expression of the *serC* (*pdxF*)-encoded transaminase, which acts between PdxB and PdxA in the de novo PLP pathway (40, 43), is minimal in rich LB medium and maximal in minimal salts-glucose medium due to opposing positive and negative controls exerted by the Lrp and cyclic AMP receptor proteins, respectively (T.-K. Man and M. E. Winkler, unpublished results) (43). However, the regulation of the SerC (PdxF) transaminase may have been strongly set by its central role in serine biosynthesis (63).

Another PLP biosynthetic gene is not subject to growth rate regulation at all. For example, PNP synthase, encoded by *pdxJ*, catalyzes ring closure of the product of the PdxA reaction to form PNP as the last step in the de novo pathway of B_6 vitamer biosynthesis (11, 26, 28, 38, 41, 44, 78). *pdxJ* is located in the complex *rnc-era-recO-pdxJ-acpS* superoperon (41, 45, 65). Extensive analyses of single-copy *pdxJ-lacZ* transcription and translation fusions indicated that *pdxJ* is not subject to growth rate regulation or to regulation by changes in fatty acid metabolism that might be expected to influence expression of the cotranscribed *acpS* gene (encodes holo-acyl-carrier protein synthase) (data not shown) (45). Understanding these diverse regulation patterns requires additional information about the cellular amounts of the PLP biosynthetic enzymes and pathway intermediates in *E. coli* growing at different rates. Another consideration is that the positive growth rate regulation in the complex superoperons that contain *pdxA* and *pdxB* (Fig. 1) may act primarily on expression of the downstream *ksgA* rRNA and *truA* (*hisT*) tRNA modification genes, respectively, which encode members of the translation apparatus. Thus, it may be that the genes encoding members of the translation apparatus, not the genes encoding PLP biosynthetic genes, are the targets of growth rate regulation in these superoperons. Consistent with this notion, *truA* (*hisT*) transcription is positively growth rate regulated in exponentially growing bacteria (69).

ACKNOWLEDGMENTS

We thank the colleagues listed in Table 1 for bacterial strains and plasmids. We thank Karen Betchel for excellent technical assistance, Genshi Zhao and Tze-Kwong Man for helpful discussions, and Gregory Robertson for help preparing the figures.

This work was supported by Public Health Service grant GM37561 from the National Institute of General Medical Sciences and resources of the Lilly Research Laboratories.

REFERENCES

1. **Aono, R., T. Negishi, and H. Nakajima.** 1994. Cloning of organic solvent tolerance gene *ostA* that determines *n*-hexane tolerance in *Escherichia coli.* Appl. Environ. Microbiol. **60:**4624–4626.
2. **Arps, P. J., and M. E. Winkler.** 1987. Structural analysis of the *Escherichia coli* K-12 *hisT* operon by using a kanamycin resistance cassette. J. Bacteriol. **169:**1061–1070.

3. **Arps, P. J., and M. E. Winkler.** 1987. An unusual genetic link between vitamin B6 biosynthesis and tRNA pseudouridine modification in *Escherichia coli* K-12. J. Bacteriol. **169:**1071–1079.
4. **Ausubel, F. M., R. Brent, R. E. Kingston, D. D. Moore, J. G. Seidman, J. A. Smaith, and K. Struhl.** 1993. Current protocols in molecular biology. Wiley-Interscience, New York, N.Y.
5. **Ball, C. A., R. Osuna, K. C. Ferguson, and R. C. Johnson.** 1992. Dramatic changes in Fis levels upon nutrient upshift in *Escherichia coli.* J. Bacteriol. **174:**8043–8056.
6. **Bartlett, M. S., and R. L. Gourse.** 1994. Growth rate-dependent control of the *rrnB* P1 core promoter in *Escherichia coli.* J. Bacteriol. **176:**5560–5564.
7. **Bartlett, M. S., T. Gaal, W. Ross, and R. L. Gourse.** 2000. Regulation of rRNA transcription is remarkably robust: Fis compensates for altered nucleoside triphosphate sensing by mutant RNA polymerases at *Escherichia coli rrn* P1 promoters. J. Bacteriol. **182:**1969–1977.
8. **Bedwell, D. M., and M. Nomura.** 1986. Feedback regulation of RNA polymerase subunit synthesis after the conditional overproduction of RNA polymerase in *Escherichia coli*. Mol. Gen. Genet. **204:**17–23.
9. **Bender, D. A.** 1985. Amino acid metabolism. John Wiley & Sons, Inc., New York, N.Y.
10. **Bremer, H., and P. P. Dennis.** 1996. Modulation of chemical composition and other parameters of the cell by growth rate, p. 1553–1569. *In* F. C. Neidhardt (ed.), *Escherichia coli* and *Salmonella*: cellular and molecular biology, 2nd ed., vol. 2. ASM Press, Washington, D.C.
11. **Cane, D. E., S. Du, J. K. Robinson, Y. Hsiung, and I. D. Spenser.** 1999. Biosynthesis of vitamin B6: enzymatic conversion of 1-deoxy-D-xylulose-5-phosphate to pyridoxol phosphate. J. Am. Chem. Soc. **121:**7722–7723.
12. **Cane, D. E., Y. Hsiung, J. A. Cornish, J. K. Robinson, and I. D. Spenser.** 1998. Biosynthesis of vitamin B6: the oxidation of 4-(phosphohydroxy)-L-threonine by PdxA. J. Am. Chem. Soc. **120:**1936–1937.
13. **Cashel, M., D. R. Gentry, V. J. Hernandez, and D. Vinella.** 1996. The stringent response, p. 1458–1496. *In* F. C. Neidhardt (ed.), *Escherichia coli* and *Salmonella*: cellular and molecular biology, 2nd ed., vol. 1. ASM Press, Washington, D.C.
14. **Castilho, B. A., P. Olfson, and M. J. Casadaban.** 1985. Plasmid insertion mutagenesis and *lac* gene fusion with mini-Mu bacteriophage transposons. J. Bacteriol. **158:**488–495.
15. **Condon, C., J. Philips, Z.-Y. Fu, C. Squires, and C. L. Squires.** 1992. Comparison of the expression of the seven ribosomal operons in *Escherichia coli*. EMBO J. **11:**4175–4185.
16. **Dakshinamurti, K. E.** 1990. Vitamin B_6. Ann. N.Y. Acad. Sci., vol. 585.
17. **Dempsey, W. B.** 1965. Control of pyridoxine biosynthesis in Escherichia coli. J. Bacteriol. **90:**431–437.
18. **Dempsey, W. B.** 1971. Control of vitamin B_6 biosynthesis in *Escherichia coli*. J. Bacteriol. **108:**415–421.
19. **Dempsey, W. B.** 1987. Synthesis of pyridoxal phosphate, p. 539–543. *In* F. C. Neidhardt (ed.), *Escherichia coli* and *Salmonella typhimurium*: cellular and molecular biology. American Society for Microbiology, Washington, D.C.
20. **Dennis, P. P., and M. Nomura.** 1975. Regulation of the expression of ribosomal protein genes in *Escherichia coli*. J. Mol. Biol. **97:**61–76.
21. **Dolphin, D., R. Poulson, and O. Avramovic (ed.).** 1986. Vitamin B_6 pyridoxal phosphate: chemical, biochemical, and medical aspects. Wiley-Interscience, New York, N.Y.
22. **Dong, H., L. A. Kirsebom, and L. Nilsson.** 1996. Growth rate regulation of 4.5 S RNA and M1 RNA the catalytic subunit of *Escherichia coli* RNase P. J. Mol. Biol. **261:**303–308.
23. **Ehrenshaft, M., P. Bilski, M. Y. Li, C. F. Chignell, and M. E. Daub.** 1999. A highly conserved sequence is a novel gene involved in *de novo* vitamin B6 biosynthesis. Proc. Natl. Acad. Sci. USA **96:**9374–9378.
24. **Emilsson, V., and L. Nilsson.** 1995. Factor for inversion stimulation-dependent growth rate regulation of serine and threonine tRNA species. J. Biol. Chem. **270:**16610–16614.
25. **Finkel, S. E., and R. C. Johnson.** 1992. The Fis protein: it's not just for DNA inversion anymore. Mol. Microbiol. **6:**3257–3265.
26. **Franco, M. G., B. Laber, R. Huber, and T. Clausen.** 2001. Structural basis for the function of pyridoxine 5′-phosphate synthase. Structure **9:**245–253.
27. **Gaal, T., M. S. Bartlett, W. Ross, C. L. Turnbough, Jr., and R. L. Gourse.** 1997. Transcription regulation by initiating NTP concentration: rRNA synthesis in bacteria. Science **278:**2092–2097.
28. **Garrido-Franco, M., R. Huber, F. S. Schmidt, B. Laber, and T. Clausen.** 2000. Crystallization and preliminary X-ray crystallographic analysis of PdxJ, the pyridoxine 5′-phosphate synthesizing enzyme. Acta Crystallogr. D Biol. Crystallogr. **56:**1045–1048.
29. **Helmreich, E. J.** 1992. How pyridoxal 5′-phosphate could function in glycogen phosphorylase catalysis. Biofactors **3:**159–172.
30. **Hill, R. E., and I. D. Spenser.** 1996. Biosynthesis of vitamin B_6, p. 695–703. *In* F. C. Neidhardt (ed.), *Escherichia coli* and *Salmonella*: cellular and molecular biology, 2nd ed., vol. 1. ASM Press, Washington, D.C.
31. **Iriarte, A., H. M. Kagen, and M. Martinez-Carrion (ed.).** 2000. Biochemistry of vitamin B_6 and PQQ-dependent proteins. Birkhäuser Verlag, Basel, Switzerland.
32. **Jensen, K. F., and S. Pedersen.** 1990. Metabolic growth rate control in *Escherichia coli* may be a consequence of subsaturation of the macromolecular biosynthetic apparatus with substrates and catalytic components. Microbiol. Rev. **54:**89–100.
33. **Jinks-Robertson, S., R. L. Gourse, and M. Nomura.** 1983. Expression of rRNA and tRNA genes in *Escherichia coli*: evidence for feedback regulation by products of rRNA operons. Cell **33:**865–876.
34. **Johnson, R. C., C. A. Ball, D. Pfeffer, and M. I. Simon.** 1988. Isolation of the gene encoding the Hin recombinational enhancer. Proc. Natl. Acad. Sci. USA **85:**3484–3488.
35. **Karlinsey, J. E., A. J. Pease, M. E. Winkler, J. L. Bailey, and K. T. Hughes.** 1997. The *flk* gene of *Salmonella typhimurium* couples flagellar P- and L-ring assembly to flagellar morphogenesis. J. Bacteriol. **179:**2389–2400.
36. **Karpeisky, M. Y., and H. B. F. Dixon.** 1986. The use of pyridoxal phosphate for modification of proteins, p. 71–116. *In* D. Dolphin, R. Poulson, and O. Avramovic (ed.), Vitamin B_6 pyridoxal phosphate: chemical, biochemical, and medical aspects, vol. B. Wiley-Interscience, New York, N.Y.
37. **Kohara, Y., K. Akiyama, and K. Isono.** 1987. The physical map of the whole *E. coli* chromosome: application of a new strategy for rapid analysis and sorting of a large genomic library. Cell **50:**495–508.
38. **Laber, B., W. Maurer, S. Scharf, K. Stepusin, and F. S. Schmidt.** 1999. Vitamin B_6 biosynthesis: formation of pyridoxine 5′-phosphate from 4-(phosphohydroxyl)-L-threonine and 1-deoxy-D-xylulose-5-phosphate by PdxA and PdxJ protein. FEBS Lett. **449:**45–48.
39. **Lam, H.-L., and M. E. Winkler.** 1992. Characterization of the complex *pdxH-tyrS* operon of *Escherichia coli* K-12 and pleiotropic phenotypes caused by *pdxH* insertion mutations. J. Bacteriol. **174:**6033–6045.
40. **Lam, H.-L., and M. E. Winkler.** 1990. Metabolic relationships between pyridoxine (vitamin B6) and serine biosynthesis in *Escherichia coli* K-12. J. Bacteriol. **172:**6518–6528.
41. **Lam, H.-L., E. Tancula, W. B. Dempsey, and M. E. Winkler.** 1992. Suppression of insertions in the complex *pdxJ* operon of *Escherichia coli* K-12 by *lon* and other mutations. J. Bacteriol. **174:**1554–1567.
42. **Lazar, S. W., M. Almiron, A. Tormo, and R. Kolter.** 1998. Role of the *Escherichia coli* SurA protein in stationary-phase survival. J. Bacteriol. **180:** 5704–5711.
43. **Man, T.-K., A. J. Pease, and M. E. Winkler.** 1997. Maximization of transcription of the *serC* (*pdxF*)-*aroA* multifunctional operon by antagonistic effects of the cyclic AMP (cAMP) receptor protein-cAMP complex and Lrp global regulators of *Escherichia coli* K-12. J. Bacteriol. **179:**3458–3469.
44. **Man, T.-K., G. Zhao, and M. E. Winkler.** 1996. Isolation of a *pdxJ* point mutation that bypasses the requirement for the PdxH oxidase in pyridoxal 5′-phosphate coenzyme biosynthesis in *Escherichia coli* K-12. J. Bacteriol. **178:**2445–2449.
45. **Matsunaga, J., M. Dyer, E. L. Simons, and R. W. Simons.** 1996. Expression and regulation of the *rnc* and *pdxJ* operons of *Escherichia coli*. Mol. Microbiol. **22:**977–989.
46. **Miller, J. H.** 1992. A short course in bacterial genetics. Cold Spring Harbor Laboratory Press, Cold Spring Harbor, N.Y.
47. **Misra, R., and P. R. Reeves.** 1987. Role of *micF* in the *tolC*-mediated regulation of OmpF, a major outer membrane protein of *Escherichia coli* K-12. J. Bacteriol. **169:**4722–4730.
48. **Mittenhuber, G.** 2001. Phylogenetic analyses and comparative genomics of vitamin B6 (pyridoxine) and pyridoxal phosphate biosynthesis pathways. J. Mol. Microbiol. Biotechnol. **3:**1–20.
49. **Morris, T. W., K. E. Reed, and J. E. Cronan.** 1995. Lipoic acid metabolism in *Escherichia coli*: the *lplA* and *lipB* genes define redundant pathways for ligation of lipoyl groups to apoprotein. J. Bacteriol. **177:**1–10.
50. **Nilsson, G., J. G. Belasco, S. N. Cohen, and A. von Gabain.** 1984. Growth rate dependent regulation of mRNA stability in *Escherichia coli*. Nature **312:**75–77.
51. **Osmani, A. H., G. S. May, and S. A. Osmani.** 1999. The extremely conserved *pyroA* gene of *Aspergillus nidulans* is required for pyridoxine synthesis and is required indirectly for resistance to photosensitizers. J. Biol. Chem. **274:** 23565–23569.
52. **Pedersen, S., P. L. Bloch, S. Reeh, and F. C. Neidhardt.** 1978. Patterns of protein synthesis in *E. coli*: a catalog of the amount of 140 individual proteins at different growth rates. Cell **14:**179–190.
53. **Petersen, C., and L. B. Moller.** 2000. Invariance of the nucleoside triphosphate pools of *Escherichia coli* with growth rate. J. Biol. Chem. **275:**3931–3935.
54. **Rasmussen, L. J., M. G. Marinus, and A. Lobner-Olesen.** 1994. Novel growth rate control of *dam* gene expression in *Escherichia coli*. Mol. Microbiol. **12:**631–638.
55. **Roa, B. B., D. M. Connolly, and M. E. Winkler.** 1989. Overlap between *pdxA* and *ksgA* in the complex *pdxA-ksgA-apaG-apaH* operon of *Escherichia coli* K-12. J. Bacteriol. **171:**4767–4777.
56. **Rose, J. K., and C. Yanofsky.** 1972. Metabolic regulation of the tryptophan operon of *Escherichia coli*: repressor-independent regulation of transcription initiation frequency. J. Mol. Biol. **69:**103–118.
57. **Rouviere, P. E., and C. A. Gross.** 1996. SurA, a periplasmic protein with peptidyl-prolyl isomerase activity, participates in the assembly of outer membrane porins. Genes Dev. **10:**3170–3182.

58. **Rowley, K. B., R. M. Elford, I. Roberts, and W. M. Holmes.** 1993. In vivo regulatory responses of four *Escherichia coli* operons which encode leucyl-tRNAs. J. Bacteriol. **175:**1309–1315.
59. **Schoenlein, P. V., B. B. Roa, and M. E. Winkler.** 1989. Divergent transcription of *pdxB* and homology between the *pdxB* and *serA* gene products in *Escherichia coli* K-12. J. Bacteriol. **171:**6084–6092.
60. **Schreiber, G., S. Metzger, E. Aizenman, S. Roza, M. Cashel, and G. Glaser.** 1991. Overexpression of the *relA* gene in *Escherichia coli*. J. Biol. Chem. **266:**3760–3767.
61. **Simons, R. W., F. Houman, and N. Kleckner.** 1987. Improved single and multicopy *lac*-based vectors for protein and operon fusions. Gene **53:**85–96.
62. **Singer, M., T. A. Baker, G. Schnitzler, S. M. Deischel, M. Goel, W. Dove, K. J. Jaacks, A. D. Grossman, J. W. Erickson, and C. A. Gross.** 1989. A collection of strains containing genetically linked alternating antibiotic resistance elements for genetic mapping of *Escherichia coli*. Microbiol. Rev. **53:**1–24.
63. **Sugimoto, E., and L. I. Pizer.** 1968. The mechanism of end product inhibition of serine biosynthesis. I. Purification and kinetics of phosphoglycerate dehydrogenase. J. Biol. Chem. **243:**2081–2089.
64. **Svitil, A. L., M. Cashel, and J. W. Zyskind.** 1993. Guanosine tetraphosphate inhibits protein synthesis *in vivo*. J. Biol. Chem. **268:**2307–2311.
65. **Takiff, H. E., T. Baker, T. Copeland, S. M. Chen, and D. L. Court.** 1992. Locating essential *Escherichia coli* genes by using mini-Tn*10* transposons: the *pdxJ* operon. J. Bacteriol. **174:**1544–1553.
66. **Tormo, A., M. Almiron, and R. Kolter.** 1990. *surA*, an *Escherichia coli* gene essential for survival in stationary phase. J. Bacteriol. **172:**4339–4347.
67. **Tosa, T., and L. I. Pizer.** 1971. Effect of serine hydroxamate on the growth of *Escherichia coli*. J. Bacteriol. **106:**966–971.
68. **Tribe, D. E., H. Camakaris, and J. Pittard.** 1976. Constitutive and repressible enzymes of the common pathway of aromatic biosynthesis in *Escherichia coli* K-12: regulation of enzyme synthesis at different growth rates. J. Bacteriol. **127:**1085–1097.
69. **Tsui, H.-C., P. J. Arps, D. M. Connnoly, and M. E. Winkler.** 1991. Absence of *hisT*-mediated pseudouridylation results in a uracil requirement that interferes with *Escherichia coli* K-12 cell division. J. Bacteriol. **173:**7395–7400.
70. **Tsui, H.-C. T., A. J. Pease, T. M. Koehler, and M. E. Winkler.** 1994. Detection and quantitation of RNA transcribed from bacterial chromosomes and plasmids, p. 179–204. *In* K. Adolph (ed.), Methods in molecular genetics: molecular microbiology, vol. 3. Academic Press, Inc., New York, N.Y.
71. **Vaisvila, R., L. J. Rasmussen, A. Lobner-Olesen, U. von Freiesleben, and M. G. Marinus.** 2000. The LipB protein is a negative regulator of *dam* gene expression in *Escherichia coli*. Biochim. Biophys. Acta **1494:**43–53.
72. **van Gemen, B., J. Twisk, and P. H. van Knippenberg.** 1989. Autogenous regulation of the *Escherichia coli ksgA* gene at the level of translation. J. Bacteriol. **171:**4002–4008.
73. **van Gemen, B., H. J. Koets, C. A. Plooy, J. Bodlaender, and P. H. van Knippenberg.** 1987. Characterization of the *ksgA* gene of *Escherichia coli* determining kasugamycin sensitivity. Biochimie (Paris) **69:**841–848.
74. **Winkler, M. E.** 2000. Genetic and genomic approaches for delineating the pathway of pyridoxal 5′-phosphate coenzyme biosynthesis in *Escherichia coli*, p. 3–10. *In* A. Iriarte, H. M. Kagen, and M. Martinez-Carrion (ed.), Biochemistry and molecular biology of vitamin B6 and PQQ-dependent proteins. Birkhäuser Verlag, Basel, Switzerland.
75. **Wolf, R. E., Jr., D. M. Prather, and F. M. Shea.** 1979. Growth rate-dependent alteration of 6-phosphogluconate dehydrogenase and glucose 6-phosphate dehydrogenase levels in *Escherichia coli* K-12. J. Bacteriol. **139:**1039–1096.
76. **Xu, J., and R. C. Johnson.** 1995. Identification of genes negatively regulated by Fis: Fis and RpoS comodulate growth-phase-dependent gene expression in *Escherichia coli*. J. Bacteriol. **177:**938–947.
77. **Zhao, G., A. J. Pease, N. Bharani, and M. E. Winkler.** 1995. Biochemical characterization of *gapB*-encoded erythrose 4-phosphate dehydrogenase of *Escherichia coli* K-12 and its possible role in pyridoxal 5′-phosphate biosynthesis. J. Bacteriol. **177:**2804–2812.
78. **Zhao, G., and M. E. Winkler.** 1996. 4-Phospho-hydroxy-L-threonine is an obligatory intermediate in pyridoxal 5′-phosphate coenzyme biosynthesis in *Escherichia coli* K-12. FEMS Microbiol. Lett. **135:**275–280.